

**PROTOTYPE DESIGN AND TESTING OF EFFICIENT METAL
PRINTED CIRCUIT BOARDS (M-PCBS) AS HEAT SINK FOR
HIGH POWER LEDS**

by

ONG ZENG YIN

**Thesis submitted in fulfilment of the requirements
for the degree of
Master of Science**

January 2016

ACKNOWLEDGEMENTS

My utmost gratitude is to my Lord almighty God whose grace and blessings are upon me through the years of my post-graduate research. Whom also provide me strength, wisdom and guidance to complete this thesis.

I would like to express my sincere gratitude and deep appreciation to my main supervisor, Assoc. Prof. Dr. Mutharasu Devarajan for his valuable guidance and big effort in supporting and motivating me throughout the whole period of the research. I also give my sincere thanks to Dr. Shanmugan Subramani for his many guidance and valuable inputs in this research project. I am most grateful with the huge financial support provided by Collaborative Research in Engineering, Science and Technology (CREST) under grant (304/PFIZIK/650601/C121) in completing this research project.

I give my special thanks to all lab technicians from Nano Optoelectronics Research Lab (NOR) for the technical support on the research equipment. Also thanks to Mohamed Mustaqim Abu Bakar from X-Ray Crystallography Lab who is helping in data acquisition. Unforgotten to give my gracious thanks to my lab colleagues who's together facing both hardness and joy in research. Thanks for the kindness and hospitality in practical works and sharing ideas and experience together throughout the years of the research.

Last but not least, a warm and utmost appreciation must be expressed to my family members for the strong love, encouragement and the financial support for my post-graduate research journey. Thank you.

Ong Zeng Yin

TABLES OF CONTENTS

	Page
Acknowledgement	ii
Table of contents	iii
List of Tables	vii
List of Figures	viii
List of Plates	xi
List of Abbreviations	xii
List of Symbols	xiii
Abstrak	xv
Abstract	xvii
CHAPTER 1 INTRODUCTION	1
1.1 Overview	1
1.2 Introduction.....	1
1.3 Problem Statement	1
1.4 Objectives	4
1.5 Research Contribution.....	4
1.6 Thesis Outline	4
CHAPTER 2 LITERATURE REVIEW	7
2.1 Overview	7
2.2 Thermal Management of Light Emitting Diodes (LEDs).....	7
2.3 Design of Printed Circuit Board (PCB) in Thermal Solution.....	9
2.4 Thin Film Coating as Effective Interface Material	10
2.5 Thin Film Deposition	12

2.6	Research Gap.....	14
CHAPTER 3 THEORETICAL BACKGROUND		16
3.1	Overview	16
3.2	Group III Nitrides	16
3.2.1	Aluminium Nitride	16
3.2.2	Boron Nitride	17
3.3	Chemical Vapour Deposition (CVD)	17
3.3.1	CVD System	17
3.3.2	Precursor Consideration	19
3.3.3	Precursor Bubbling Method	20
3.4	Principle of 1-D Heat Transfer	21
3.5	Thermal and Optical Relation in Thermal Measurements	23
CHAPTER 4 METHODOLOGY		25
4.1	Overview	25
4.2	Thin Film Synthesis	26
4.2.1	Substrates' Preparation	26
4.2.2	DC & RF Co-Sputtering Technique.....	27
4.2.3	Chemical Vapour Deposition (CVD) Technique	29
4.2.3.1	Ceramic Tube Furnace System	30
4.2.3.2	Combined Furnaces System	31
4.2.3.3	Precursor Bubbling System	31
4.3	Structural Characterizations	34
4.3.1	X-Ray Diffraction Analysis	35
4.3.2	Surface Topography Analysis	36

4.4	Prototype PCB Fabrication	36
4.5	Thermal Characterization	38
4.5.1	Thermal Measurement – <i>Thermal Substrates</i>	40
4.5.2	Thermal Measurement – <i>Prototype M-PCBs</i>	41
4.6	Optical Characterization	42
4.6.1	Spectrometer Measurement	42
4.6.2	Industrial Optical Measurement	43
CHAPTER 5 RESULTS AND DISCUSSION		44
5.1	Overview	44
5.2	Experimental Observations of CVD Process	44
5.2.1	Ceramic Tube Furnace System	45
5.2.2	Combined Furnaces System	46
5.2.3	Precursor Bubbling System	47
5.3	XRD Results of B-AlN Thin Film Coated Al Substrates	47
5.3.1	XRD Spectra of B-AlN by Co-Sputtering Method	48
5.3.2	XRD Spectra of Thin Film by CVD Method (Gas Flow Rate)	49
5.3.3	XRD Spectra of Thin Film by CVD Layer Stacking Method	50
5.3.4	Structure Properties of B-AlN Thin Films	51
5.4	AFM Results of B-AlN Thin Film Coated Al Substrates	55
5.5	Thermal Characterization	58
5.5.1	Thermal Measurement Results of <i>Thermal Substrates</i>	58
5.5.1.1	Total Thermal Resistance of LED System with <i>Thermal Substrates</i>	59
5.5.1.2	Substrate Thermal Resistance of	

	<i>Thermal Substrates</i>	61
5.5.1.3	Rise in Junction Temperature of LED on <i>Thermal Substrates</i>	62
5.5.2	Thermal Measurement Results of <i>Prototype M-PCBs</i>	64
5.5.2.1	Total Thermal Resistance of LED on <i>M-PCBs</i>	65
5.5.2.2	PCB Thermal Resistance of <i>M-PCBs</i>	67
5.5.2.3	Rise in Junction Temperature of LED on <i>M-PCBs</i>	68
5.6	Optical Characterization	70
5.6.1	Optical Results of Thermal Substrates	70
5.6.1.1	Optical Behaviour with Various Driving Currents of <i>Thermal Substrates</i>	71
5.6.1.2	Illuminance of 3W Green LED Package on <i>Thermal Substrates</i>	72
5.6.2	Optical Results of <i>Prototype M-PCBs</i>	74
5.6.2.1	Correlated Colour Temperature (CCT) of LED on <i>M-PCBs</i>	75
5.6.2.2	Illuminance of LED on <i>M-PCBs</i>	76
5.7	Performance Comparison of <i>Prototype M-PCBs</i> with MCPCB	77
5.7.1	Thermal Performance Comparison	78
5.7.2	Optical Performance Comparison	81
	CHAPTER 6 CONCLUSIONS	88
6.1	Conclusions of the Study	88
6.2	Recommendations for Future Research.....	89
	REFERENCES	93
	APPENDICES	103
	LIST OF PUBLICATIONS	116

LIST OF TABLES

		Page
Table 2.1	Thermal resistance (R_{th}) of various interface material on Cu substrates	11
Table 4.1	Process parameters of co-sputtering depositions	28
Table 4.2	Various gas flow rates of CVD process	33
Table 4.3	Average thickness of B-AlN multi-layers	34
Table 4.4	Average Thickness of screen printed PCB layers	38
Table 5.1	XRD analysis data of B-AlN thin films	52
Table 5.2	Structural properties of c-AlN peak from various processes	53
Table 5.3	Summarized R_{th-sub} of <i>Thermal Substrates</i>	62
Table 5.4	Summarized R_{th-sub} of <i>M-PCBs</i>	67
Table 5.5	Summarized CRI values of LED on <i>Thermal Substrates</i>	71
Table 5.6	Summarized CRI values of LED on <i>M-PCBs</i>	74
Table 5.7	Structural comparison of MCPCB and <i>M-PCB</i>	77

LIST OF FIGURES

		Page
Figure 1.1	Structure of typical PCB: (a) FR4 PCB, (b) MCPCB	2
Figure 1.2	Simulated heat flow and T_j of (a) FR4 PCB, (b) MCPCB	3
Figure 2.1	One dimensional heat flow path in a typical high power LED system	8
Figure 2.2	Thermal resistance model of LED system	9
Figure 2.3	Schematic structure of <i>Super</i> MCPCB and MCPCB by N. Wang et al.	9
Figure 2.4	Cumulative structural function of MCPCB and Al_2O_3 deposited MCPCB by H.M. Cho et al.	10
Figure 2.5	Thermal resistance (R_{th}) comparison of BN coated Cu substrate with different boundary conditions	11
Figure 2.6	Cumulative structural function of LED mounted on Al substrate with various interface boundary conditions	12
Figure 2.7	Schematic diagram of molecular beam epitaxy (MBE)	13
Figure 2.8	Schematic diagram of sputtering process	13
Figure 3.1	Typical set-up of a CVD system	18
Figure 3.2	CVD reaction kinetics of in reaction zone	19
Figure 3.3	The flow mechanism of liquid precursor bubbler	21
Figure 3.4	One dimension heat transfer across a material	21
Figure 3.5	TIM applied to fill up the air gaps between two materials	22
Figure 4.1	Process flow chart of research methodology	25
Figure 4.2	Synthesis processes of B-AlN thin film depositions	26
Figure 4.3	Set-up of DC & RF Sputtering Process	27
Figure 4.4	The chronology of precursor choices and CVD set-ups in optimization of CVD process	30
Figure 4.5	Schematic diagram of three zone ceramic tube CVD system	30

Figure 4.6	Schematic diagram of three zone and single zone quartz tube combined CVD system	31
Figure 4.7	Schematic diagram of precursor bubbling method of CVD system	32
Figure 4.8	Schematic diagram of multi-layer stacked thin films on Al substrate	34
Figure 4.9	The process flow of PCB fabrication by screen printing	36
Figure 4.10	Design model of prototype <i>M-PCB</i>	37
Figure 4.11	Golden Dragon white LED mounted on <i>M-PCB</i>	38
Figure 4.12	Schematic diagram of 3W green LED package mounted on <i>Thermal Substrate</i>	40
Figure 4.13	K-factor of 3W green LED package	41
Figure 4.14	Schematic diagram of Golden Dragon White LED mounted on <i>M-PCB</i>	41
Figure 4.15	Optical measurement set-up of DUT in still air chamber	42
Figure 5.1	XRD spectra of co-sputtered B-AlN thin films by various processes	48
Figure 5.2	XRD spectra of B-AlN thin films deposited by various CVD processes	50
Figure 5.3	XRD spectra of B-AlN thin films deposited layer stack method	51
Figure 5.4	Crystallite size of c-AlN peak from various processes	54
Figure 5.5	3D surface images of B-AlN thin films by various processes	56
Figure 5.6	Surface roughness of B-AlN by various processes	57
Figure 5.7	Schematic diagram of 3W LED mounted on <i>Thermal Substrate</i>	58
Figure 5.8	Cumulative structure function measured LED package on <i>Thermal Substrate</i>	59
Figure 5.9	Total thermal resistances (R_{th-tot}) of <i>Thermal Substrates</i> by various processes	60
Figure 5.10	Rise in junction temperature of <i>Thermal Substrates</i>	63
Figure 5.11	Schematic diagram of <i>M-PCB</i>	64

Figure 5.12	Cumulative structural function of LED on <i>M-PCB</i>	64
Figure 5.13	Total thermal resistances (R_{th-tot}) of <i>M-PCBs</i> by various processes	66
Figure 5.14	Rise in junction temperature of <i>M-PCBs</i>	69
Figure 5.15	Variation of LUX level in 15 minutes of LED on <i>Thermal Substrates</i>	72
Figure 5.16	LUX level of LED package on <i>Thermal Substrates</i>	73
Figure 5.17	CCT comparison of <i>M-PCBs</i> at various driving currents	75
Figure 5.18	LUX level of LED package on <i>M-PCBs</i>	76
Figure 5.19	Cumulative structural function of LED on various PCBs	78
Figure 5.20	R_{th-tot} comparison of MCPCB with <i>M-PCBs</i>	79
Figure 5.21	R_{th-pcb} comparison of MCPCB with <i>M-PCBs</i>	79
Figure 5.22	ΔT comparison of LED on various PCBs	81
Figure 5.23	CCT comparison of MCPCB and <i>M-PCBs</i> at various driving currents	82
Figure 5.24	The LUX level comparison of MCPCB and <i>M-PCBs</i> at various driving current.	82
Figure 5.25	A. Luminous flux and, B. Efficacy of LED on various PCBs	83
Figure 5.26	CIE 1931 colour coordinate plot of LED on PCBs at 100 mA	84
Figure 5.27	CIE 1931 colour coordinate plot of LED on PCBs at 350 mA	85
Figure 5.28	CIE 1931 colour coordinate plot of LED on PCBs at 700 mA	85
Figure 6.1	Reaction kinetics of (a) Thick and (b) Thin boundary layers	91
Figure 6.2	Simulated flow of current CVD process	92
Figure 6.3	Simulated flow of suggested substrates' holder	92

LIST OF PLATES

		Page
Plate 4.1	Al substrate (Grade 1045)	27
Plate 4.2	CVD furnaces: (a) Three zone ceramic tube furnace, (b) Single zone furnace, (c) Three zone quartz tube furnace	29
Plate 4.3	Thermal Transient Tester (T3Ster, Mentor Graphics)	38
Plate 4.4	Thermal characterisation of DUT in still air chamber	39
Plate 4.5	LED Spectrometer (MK350, UPRtek)	42
Plate 4.6	Pentamaster LEDster IV	43
Plate 5.1	The surface condition of various substrates after high temperature process	44
Plate 5.2	Quartz tube condition after CVD process	45
Plate 5.3	White adduct covered the cool zone of quartz tube	46
Plate 5.4	Defects found from PCB fabrication	65

LIST OF ABBREVIATIONS

LED	Light emitting diode
PCB	Printed circuit board
MCPCB	Metal core printed circuit board
TIM	Thermal interface material
BLT	Bond line thickness
XRD	X-ray diffraction
AFM	Atomic force microscope
FESEM	Field emission scanning electron microscope
DUT	Device under Test
<i>M-PCB</i>	Metal-printed circuit board
CCT	Correlated colour temperature
CRI	Colour rendering index
LUX	Illuminance

LIST OF SYMBOLS

R_{th}	Thermal resistance
T_J	Junction temperature
ΔT_J	Rise in junction temperature
Q	Heat source
T	Temperature
A	Cross-sectional area
k	Thermal conductivity
k_{TIM}	Thermal conductivity of TIM
$R_{effective}$	Effective thermal resistance
R_c	Contact resistance
P_I	Input electrical power
P_{opt}	Output optical power
P_H	Heat dissipation power
$P_{thermal}$	Thermal power
V	Forward voltage
D	Crystallite size
λ	Wavelength of radiation
β	Full width at half maximum (FWHM)
θ	Bragg diffraction angle of (hkl)
σ	Internal stress
d	d-spacing
E	Young's modulus
Y	Poisson's ratio

ε	Micro-strain
R_a	Surface roughness
I_{tot}	Total current
I_{sc}	Sensor current
I_{in}	Input current
ΔV_F	Difference in temperature-sensing voltage
K	Sensitivity value (K factor)
R_{th-tot}	Total thermal resistance
R_{th-sub}	Substrate thermal resistance
R_{th-pcb}	PCB thermal resistance

REKA BENTUK PROTOTAIP DAN UJIAN BAGI PAPAN LITAR BERCETAK LOGAM (M-PCBS) YANG CEKAP SEBAGAI SINK HABA UNTUK LEDS KUASA TINGGI

ABSTRAK

Dalam penyelesaian cabaran haba diod pemancar cahaya (LED) beroperasi, suatu penyiasatan atas reka bentuk papan litar bercetak (PCB) haba cekap telah menarik perhatian banyak industri. Papan litar bercetak berteras logam (MCPCB) telah menjadi pilihan yang sangat baik. Walaupun ia merupakan penyebar haba yang sangat baik dalam mengurangkan suhu berlebihan pada simpang LED, fabrikasi MCPCB melibatkan pelbagai langkah proses dan beberapa lapisan. Lebih banyak lapisan PCB mewujudkan rintangan haba (R_{th}) tinggi yang disumbangkan oleh beberapa lapisan antara muka. Oleh itu, mengenal pasti bahan konduktif haba yang tinggi pada substrat logam dengan lapisan antara muka yang minimum untuk pemindahan haba yang lebih baik dan operasi LED yang cekap. Dalam kajian ini, boron doped aluminium nitride (B-AlN) filem nipis pada Al substrat telah disediakan oleh dua jenis teknik yang berlainan iaitu permecikan bersama arus terus (DC) dengan frekuensi radio (RF) dan penmendapan wap kimia (CVD) bersuhu rendah pada tekanan atmosfera dengan precursor alternatif. Parameter sintesis telah diubah dan dioptimumkan untuk mendapatkan kualiti B-AlN filem nipis yang baik. Antara teknik sintesis, filem yang disediakan oleh kaedah CVD menunjukkan sifat-sifat struktur yang lebih baik dan telah dipilih untuk fabrikasi PCB prototaip. Sebelum fabrikasi PCB, Al substrat dilapisi B-AlN telah diuji prestasi terma dan optik sebagai sink haba (*Thermal Substrates*) dengan menggunakan kaedah analisis fana LED kuasa tinggi dan LED spektrometer. Beberapa prototaip PCB (*M-PCBs*) akhirnya dibina pada Al substrat dilapisi B-AlN dan diuji prestasi terma dan optik dengan LED kuasa tinggi yang dipasang pada prototaip. Perbandingan antara *M-PCB* dengan

MCPCB komersial menunjukkan bahawa *M-PCB* disediakan daripada B-AlN filem nipis dilapisi dengan paramter proses CVD (**CVD 4**) mempunyai prestasi terma yang lebih baik daripada MCPCB pada keadaan operasi yang sama. Pada arus elektrik 700 mA, M-PCB ketara mencapai R_{th-tot} dan R_{th-pcb} yang lebih rendah berbanding dengan MCPCB. Kenaikan suhu simpang (ΔT_J) telah dikawal dan dikurangkan secara drastik dari 65.77 °C ke 52.55 °C bagi kegunaan M-PCB berbanding dengan MCPCB. Nilai suhu warna berhubung kait (CCT) LED pada *M-PCB* diuji dengan 700 mA adalah lebih rendah (≈ 8100 K) bila berbanding dengan MCPCB komersial (≥ 10000 K) dan warna cahaya dieleakkan beralih kepada warna “biru”. Didapati bahawa *M-PCB* juga menunjukkan peningkatan fluks cahaya (68.38 lm) berbanding dengan MCPCB (61.83 lm).

PROTOTYPE DESIGN AND TESTING OF EFFICIENT METAL PRINTED CIRCUIT BOARDS (M-PCB) AS HEAT SINK FOR HIGH POWER LEDS

ABSTRACT

In solving the thermal challenges in LED operation, an investigation on designing the thermally efficient printed circuit board (PCB) has drawn the attention of many industries. Metal-core printed circuit board (MCPCB) has been an excellent choice. Though it is an excellent heat spreader in reducing the excessive temperature at the LED junction, the fabrication of MCPCB involves various process steps and number of layers. More PCB layers create high thermal resistance (R_{th}) which is contributed by several interface layers. Therefore, it is necessary to identify high thermal conductive material on metal substrate with minimal interface layers for better heat transfer and efficient LED operation. In this research, boron doped aluminium nitride (B-AlN) thin films on Al substrates were prepared by two different techniques which are DC & RF co-sputtering and low temperature chemical vapour deposition (CVD) at atmospheric pressure with alternative precursor. The synthesis parameters were varied and developed to obtain good quality B-AlN thin film. Among the synthesis techniques, films prepared by CVD method showed better structural properties and were chosen for fabrication of prototype PCBs. Prior to the PCB fabrication, B-AlN coated Al substrates were tested for their thermal and optical performances as heat sink (*Thermal Substrates*) using transient analysis method of the high power LED and LED spectrometer. Several prototype PCBs (*M-PCBs*) were eventually fabricated on B-AlN coated Al substrates and tested for their thermal and optical performances with high power LEDs mounted on prototypes. The comparison between *M-PCB* and commercial MCPCB had shown that the *M-PCB* prepared from B-AlN thin film coated by CVD process (**CVD 4**) had better thermal performance than MCPCB. At 700 mA driving current, *M-PCB* significantly achieved lower R_{th-tot}

and R_{th-pcb} as compared to MCPCB under the same operating condition. The rise in junction temperature of LED (ΔT_j) was controlled and reduced drastically from 65.77 °C to 52.55 °C by using *M-PCB* as compared to that with MCPCB. The correlated colour temperature (CCT) value of the LED on *M-PCB* at 700 mA was lower (≈ 8100 K) when compared with commercial MCPCB (≥ 10000 K) and avoided the colour shifting towards “bluish” colour. It was found that *M-PCB* also showed increased luminous flux (68.38 lm) as compared with MCPCB (61.83 lm).

CHAPTER 1

INTRODUCTION

1.1 Overview

The chapter includes a brief introduction to thermal challenges in LEDs, the current problem faced in this field, the contribution and output of the project, the research objectives and the outline of the whole thesis.

1.2 Introduction

Light Emitting Diode (LED) is a low energy consumption semiconductor light source. In the advancement of the luminescence technology, the evolution of LED has great impact in lighting solutions over the years. It provides better optical performance than incandescent/halogen light with the efficiency of visible light output can be improved to approximately 10-20 %, and it has much longer lifetime than traditional light source [1-2].

However, the miniaturization of LED package design with the increase in current density has challenged the thermal management of LED. The heat dissipation through small size devices can be more than their predecessors which have larger package size. Approximately 70-90 % of energy is converted into heat in LED package [3-4]. Thus, better thermal management techniques must be implemented to dissipate the large amount of heat from the package.

1.3 Problem Statement

Thermal impedance between the components and PCB is the main issue in solid state lighting, which may contribute high thermal resistance (R_{th}) and excessive rise in junction temperature (ΔT_j) of LED packaging. Consequently, it will negatively affect

the lifetime, brightness, and colour uniformity of the light output, excessive T_j may also lead to device damage or failure [5-6]. Thus, thermal management of high power devices like LEDs has become more and more critical aspect of LED system design.

In order to overcome the thermal problem, sufficient heat removal is essential from LED chip to ambient. The design in structure and thermal conductive material of Printed Circuit Boards (PCBs) is suggested for thermal management in solid state lighting. One of the popular approaches to compensate the thermal problem in PCB is the design of Metal Core Printed Circuit Board (MCPCB), which consists of thick metal base substrate, thin dielectric layer and the circuitry layer. FR4 PCB consists of copper layers cladded on top and bottom of thick FR4 substrate. The structures of typical FR4 PCB and MCPCB are presented in Fig. 1.1. The thermal performance comparison of both FR4 PCB and MCPCB in terms of T_j obtained from simulation software (Mentor Graphics FloEFD 11) is shown in Fig. 1.2.

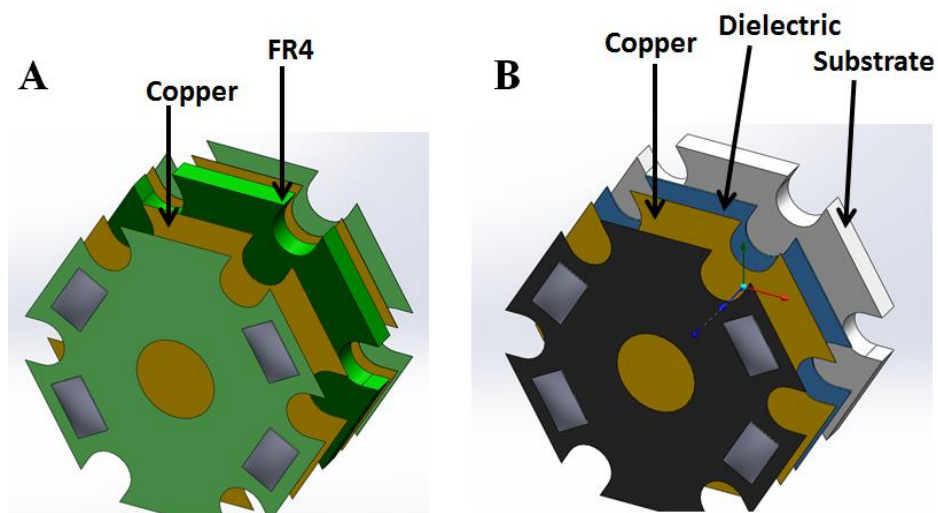


Figure 1.1 Structure of typical PCB: A. FR4 PCB, B. MCPCB

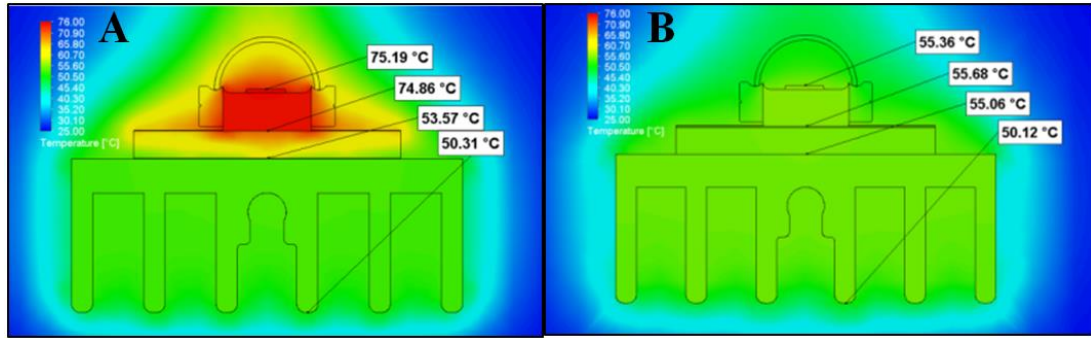


Figure 1.2 Simulated heat flow and T_j of: A. FR4 PCB, B. MCPCB

At 1 W of heat source generated on the LED chip, the results from the simulation show that MCPCB performs better in removing heat from junction to ambient. Due to low thermal conductivity of thick FR4 layer, the heat is trapped at the heat slug of the LED package. Since the advantage of MCPCB is the thick metal substrate, the dielectric material has become the key property which will determine the thermal effectiveness of MCPCB. Therefore, to meet the increasing demand of thermal requirement of the high power dissipation PCBs, it is vital to improve the thermal path of PCBs by suggesting and designing new structure and material of PCB.

Thin film coating is suggested as interface material and also heat spreader to enhance the thermal path of PCB and chemical vapour deposition (CVD) method is proposed for thin film synthesis in this project. However the CVD synthesis of nitride thin film on metal substrate has not been reported so far due to high temperature requirement (≥ 800 °C), which is not suitable for metal substrates with low melting point. Therefore, alternative CVD method has to be established in attempt to deposit nitride thin film on metal substrate.

1.4 Objectives

There are three objectives to achieve in this study:

- *To synthesize Boron doped Aluminium Nitride (B-AlN) thin film layer on Aluminium (Al) substrates using DC/RF co-sputtering and Chemical Vapour Deposition (CVD) methods with varying their parameters.*
- *To investigate the thermal and optical performances of LED package with B-AlN thin film coated Al substrate as efficient heat sink.*
- *To design and fabricate a prototype metal PCB (M-PCB) with B-AlN thin film coated Al substrate and compares the thermal and optical performances of LED between MCPCB and M-PCB.*

1.5 Research Contribution

As the outcome of this project, a ceramic thin film coated prototype Metal-PCB (M-PCB) for high power LED is delivered. In addition, the low cost CVD synthesis technique of thin film coating on metal substrate is developed for PCB fabrication industries.

1.6 Thesis Outline

This thesis is divided into six major chapters, which are introduction, literature review, theoretical background, methodology, results and discussion, and conclusion.

i) Chapter 1 : Introduction

This first chapter provides general introduction about LED and importance of thermal management in high power LED. Then followed by the problem statement which states the issues with LED heat

dissipation that lead to this research. The objectives are presented and it also includes research contribution of the project.

ii) Chapter 2 : Literature Review

This second chapter presents the literatures of the LED thermal management, some research backgrounds of PCBs, thermal applications of thin film and deposition methods with CVD and other related processes, and includes the reviews of all the previous works which had been done or discovered by other people and authors. Besides, the advantages and disadvantages of some common synthesis methods such as CVD, PVD, and Molecular Beam Epitaxy (MBE) are discussed.

iii) Chapter 3 : Theoretical Background

In third chapter, the general introduction of group III nitrides thin films is discussed. The CVD system and process are discussed extensively here. The descriptions of the thermal and optical performances of LED are also included in this chapter.

iv) Chapter 4 : Methodology

This chapter describes in the methodology of this project, which begins with substrates preparation, process development, PCB fabrication, LED characterization and data analysis.

v) **Chapter 5 : Results and Discussion**

This chapter presents the results of the data collected from the thin film analysis and LED thermal and optical characterizations. The results are also presented in forms of graphics and figure from analysis equipment.

vi) **Chapter 6 : Conclusions and Recommendations**

In this last chapter, the results of the work are summarized and conclusions are presented. Future suggestions and recommendations to enhance and further carry out this research are also included in this chapter.

CHAPTER 2

LITERATURE REVIEW

2.1 Overview

This chapter presents the concept and mechanism of heat transfer and thermal management of LED packages. The studies and reports of researches on enhancement of heat dissipation in high power devices are also included. The focuses of this chapter are:-

- *Thermal Management of LED System*
- *Designs of Printed Circuit Board (PCB) in Thermal Solution*
- *Thin Film Coating as Effective Interface Material*
- *Thin Film Deposition Methods*

2.2 *Thermal Management of Light Emitting Diodes (LEDs)*

When power is applied on LED chip, luminescence reaction occurs at the p-n junction semiconductor material and only a portion of energy is converted into light output. The rest of the energy is then turn into the form of heat which must be removed from the LED chip. Unlike traditional incandescent bulbs, LED does not radiate heat; thermal conduction is the only way to dissipate the excessive heat [7]. Fig. 2.1 describes the heat conduction in typical high power LED from p-n junction to the PCB followed by external heat sink into the ambient.

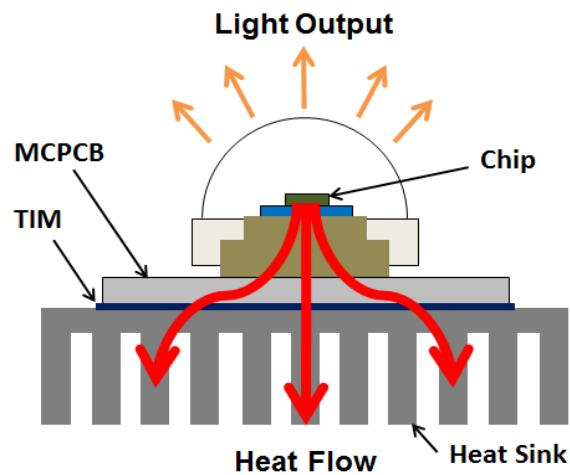


Figure 2.1 One dimensional heat flow path in a typical high power LED system

In general, the higher the input power, the greater the amount of heat generated at the LED chip. Proper thermal path must be established in order to remove the great amount of heat effectively from the chip into the surrounding through conduction. LEDs' chip today can only endure up to 150 °C [8]. Heat must be removed properly from LED chip to ambient in order to maintain the expected lifetime, light output and colour.

To describe the thermal system of LED package, the system can be simplified and illustrated using thermal resistance model as shown in Fig 2.2 [9]. The model is analogous to an electrical circuit, where heat source (Q) is represented by current source, heat flow is represented by current, the voltage is represented temperature (T), and resistor is represented the thermal resistance (R_{th}).

The two basic parameters to evaluate LED performance are junction temperature (T_j) and thermal resistance (R_{th}). The heat generation at the p-n junction has the highest temperature in LED package which is the T_j . The capability of heat transfer across the whole LED system determines the T_j of the LED chip. So the major impact of LED performance lies on the design of thermal path from chip to ambient.

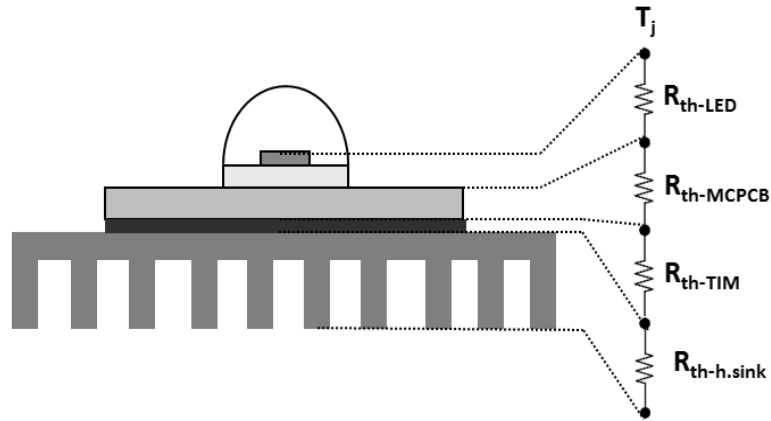


Figure 2.2 Thermal resistance model of LED system

2.3 Design of Printed Circuit Board (PCB) in Thermal Solution

There are several works on designing thermal efficient PCB have been reported in literature. Wang et al. [10] evaluated the thermal performance of Direct Plated Copper (DPC) ceramic substrate and custom designed *Super*MCPCB with extended heat spreader as shown in Fig. 2.3, which shows better performance than conventional MCPCB. There is another work on designing DPC ceramic spreader which also shows better performance over MCPCB [11].

It was reported by Shen et al. [12] that with 30 % diamond powder filled dielectric layer has 36 % reduction of R_{th} as compared to typical MCPCB. It is also reported of using high thermal conductive nitride fillers for the improvement of thermal conductivity [13]. Besides that, reduction in R_{th} of 4-5 K/W is reported on MCPCB with dense alumina thin film deposited by aerosol deposition method as presented in Fig. 2.4 [14].

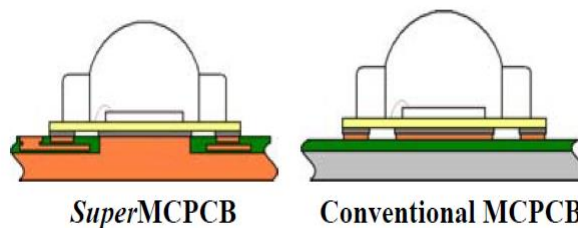


Figure 2.3 Schematic structure of *Super*MCPCB and MCPCB by Wang et al. [10]

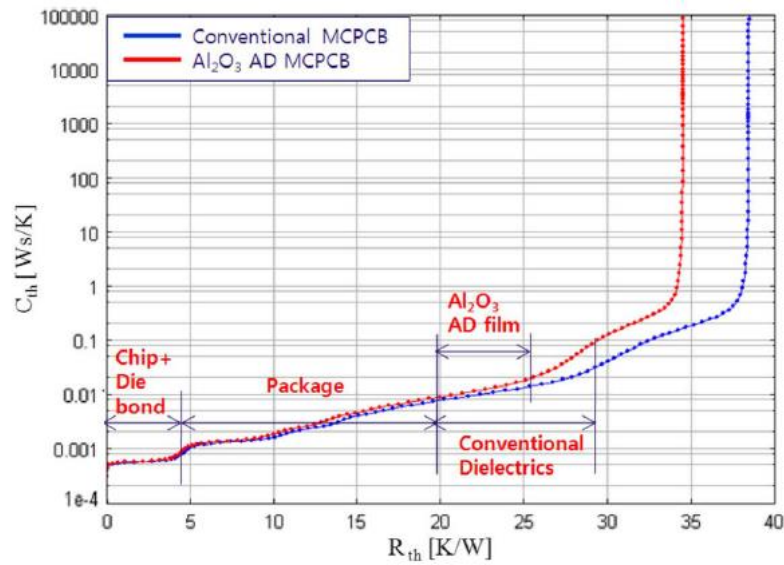


Figure 2.4 Cumulative structural function of MCPCB and Al₂O₃ deposited MCPCB by Cho et al. [14]

2.4 Thin Film Coating as Effective Interface Material

In designing effective thermal system in high power devices, heat sink has become the key component. Works on designing effective heat sinks had been carried out in order to dissipate heat from device into ambient [15-17]. However, the contact area between LED package and heat sink has significant effect on the thermal path of whole system [18]. Thermal interface material (TIM) has been the common solution in this issue [19] and grease has been a popular type of TIM in increase total contact area between two materials [20,21].

There are several works reported on the use of thin film as effective TIM for LED system at noticeable improvement is achieved at high driving current. Before this project, some preliminary research works were done on sputtered AlN [22] and BN [23] thin films on Cu substrates as TIM of heat sink for high power LED. The evidences of improvement in thermal performance are shown in Table 2.1 and Fig. 2.5, the R_{th} values of AlN and BN coated Cu substrate are lower as compare with bare substrate and thermal paste applied substrate.

Table 2.1 Thermal resistance (R_{th}) of various interface material on Cu substrates [22]

Driving Current (mA)	100	350	700
LED/Cu	38.35	37.72	35.32
LED/TP/Cu	38.06	36.87	35.89
LED/AlN/Cu	36.42	35.80	33.05

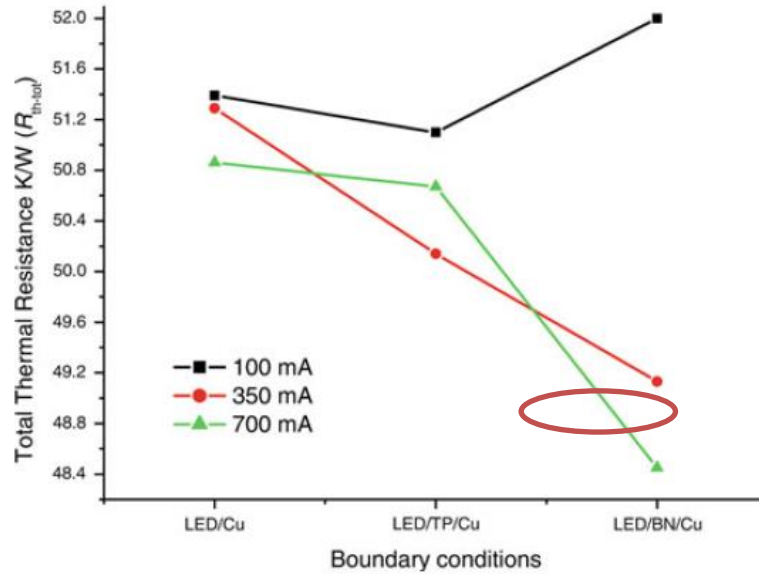


Figure 2.5 Thermal resistance (R_{th}) comparison of BN coated Cu substrate with different boundary conditions [23]

Later work on AlN thin film was also conducted on Al substrate by sputtering process [24]. From the results of transient measurements shown in Fig. 2.6, it clearly shows that all AlN coated Al substrates have lower R_{th} values as compare with substrates with and without using thermal paste.

Other work conducted by Chowdhury et al. [25] on designing a superlattice-based thin film thermoelectric cooler for a test chip reported the cooling as much as 15 °C at the targeted region of Si test chip. In reference to the evidences reported, B-AlN thin film is proposed for LED cooling which is deposited by CVD method.

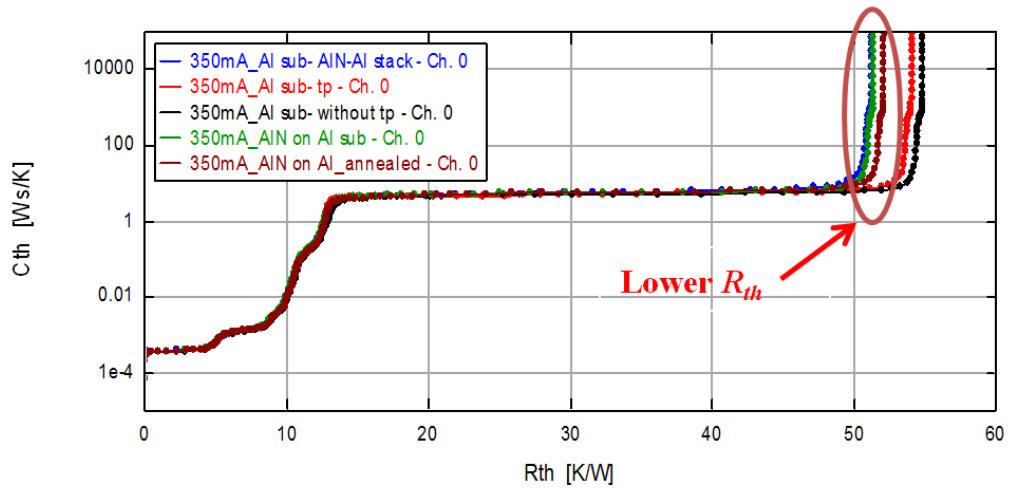


Figure 2.6 Cumulative structural function of LED mounted on Al substrate with various interface boundary conditions [24]

2.5 Thin Film Deposition

Since many years, a variety of fabrication methods for AlN and BN thin films had been reported. The common deposition techniques used in industry to synthesize thin films are Sputtering [26-28], Molecular Beam Epitaxy (MBE) [29], Pulsed Laser Deposition (PLD) [30,31], and Chemical Vapour Deposition (CVD) [32-34].

The MBE method (as shown in Fig. 2.7) gives the most precise control of the thickness layer uniformity and doping, and it can produce highly abrupt junction between different materials under low temperature with low percentage of defects [35]. However, the cost is the most expensive among all the deposition methods and it does not scale well for industrial production.

Sputtering and PLD are both physical vapour deposition (PVD) where the film thickness and ally composition can also be controlled by fixing the operating parameters and adjusting the deposition time. The basic sputtering process is shown in Fig. 2.8. The main drawback in PVD method is low deposition rate due to the limitation of power input on the target material.

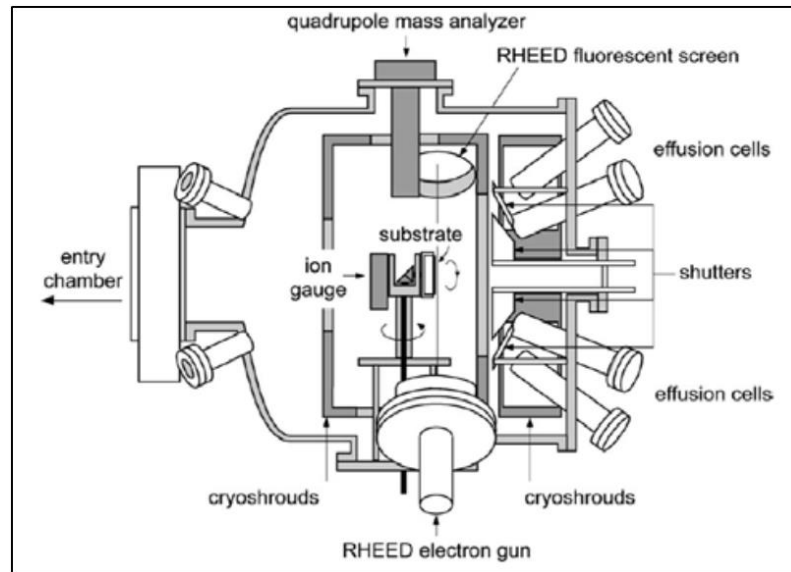


Figure 2.7 Schematic diagram of molecular beam epitaxy (MBE) [35].

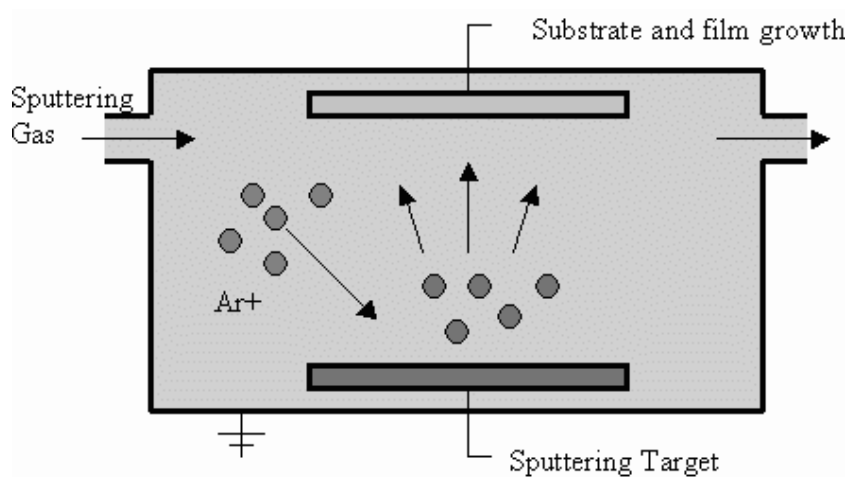


Figure 2.8 Schematic diagram of sputtering process [36]

On the other hand, CVD has the advantages over MBE and PVD in terms of overall cost and high deposition rate. CVD reactor is relatively simple which can be modified to accommodate higher number of substrates, and it does not require ultra-high vacuum condition as in PVD. Another benefit of CVD is that it generally can be adapted to many process variations for synthesis of different materials [37,38]. Film formation relies upon the chemical reaction of precursors [39]. So CVD method is the preferred choice in current reserach for the synthesis of B-AlN thin film.

In nitride CVD deposition, ammonia gas (NH_3) has been the common nitrogen source for nitride growth in CVD process [40,41]. However, high deposition temperature (typically ≥ 1000 °C) is required due to high thermal stability of NH_3 . Moreover the gas is toxic and requires proper exhaust system. The high temperature seriously limits the choice of substrate material available as the substrate is positioned at the highest temperature of deposition zone [42].

In attempt to reduce the deposition temperature, plasma-enhanced CVD (PECVD) had been suggested [43,44] where plasma activated reactions can occur at lower deposition temperature. However this technique is difficult to control and the system is expensive. In addition, metal organic CVD (MOCVD) method has been widely adopted to produce high quality nitride films [45,46]. The use of metal-organic precursors such as hexakis(dimethylamido)dialuminum [$\text{Al}_2(\text{NMe}_2)_6$] [47] and trimethylaluminum [$\text{Al}_2(\text{CH}_3)_6$] [48] have been developed to surmount the high temperature problem, but the precursors are not easy to handle and not stable in the presence of oxygen and moisture. There are some reports on utilizing attractive single-source precursor such as trimethylaluminium ammonia [$(\text{Me}_3\text{Al}(\text{NH}_3))$] adduct [49,50]. However the preparation of single-source precursors involves complex and costly procedures.

2.6 Research Gap

In this work, the deposition temperature must be low (< 650 °C) to prevent the melt of metal substrates in the synthesis of B-AlN thin films. In reference to the reports on successive use of mixed precursor with *Tert*-buthylamine (${}^t\text{BuNH}_2$) at lower deposition temperature (400 – 600 °C) [51,52], the CVD method was developed through the utilization of liquid ${}^t\text{BuNH}_2$ precursor as alternative

independent nitrogen source with better vapour pressure (340 Torr at 25 °C) [53] instead of high thermal stable NH_3 .

In order to further enhance the thermal conductivity of AlN, boron was chosen as dopant for AlN thin film. Some literatures reported that addition of Cr [54,55] and Si [56] as dopant can enhance the properties of AlN, and some reported that addition of Zr [57] and B [58] can improve the thermal conductivity of composite materials. Very few works were conducted on combination of group III elements as dopant in nitride film and they proved that boron doping can shrink the lattice of AlN structure and thus improves the thermal conductivity [59,60]. In this work, boron was introduced as dopant through the use of boron trichloride (BCl_3) precursor in deposition of B-AlN thin films.

CHAPTER 3

THEORETICAL BACKGROUND

3.1 Overview

This chapter focus on the introduction of group III nitrides on their characteristics and applications of the field. The overall view of chemical vapour deposition (CVD) in its principles, technology and mechanism is presented here. The basic theory of thermal and optical relation in thermal resistance is also explained here.

3.2 Group III Nitrides

Group III-Nitride semiconductor materials like (Al, In, Ga)N are materials that have excellent wide band gap semiconductors which are highly recommended for modern electronic and optoelectronic applications [61]. Recent research results related to AlN, BN and InN are reviewed, focusing on the different growth techniques of Group III-nitride crystals and epitaxial films, heterostructures and devices.

3.2.1 Aluminium Nitride

Aluminium nitride (AlN) is one of the most attractive non-oxide ceramic materials of group-III nitrides. It is famous because of its unique properties such as good electrical resistivity ($10^{14} \Omega\text{cm}$) due to high energy gap (6.2 eV), high breakdown voltage (15 kV/mm), low thermal expansion coefficient, high mechanical strength, high thermal conductivity [$260\text{W}/(\text{mK})$], high melting point and also high corrosion resistance [62].

Theoretically the thermal conductivity of AlN is reported to be about $280 \text{Wm}^{-1}\text{K}^{-1}$ [63]. Kuo et al. [64] reported that the value of AlN thin film is lower at the range of $0.4 - 26 \text{Wm}^{-1}\text{K}^{-1}$. Another research reported thermal conductivity of

170 Wm⁻¹K⁻¹ was achieved in AlN thin film [65]. The thermal conductivity is very much depending on the deposition method and process conditions that affect the film properties.

3.2.2 Boron Nitride

Boron Nitride BN is another attractive nitride material which has high thermal conductivity, chemical inertness, very high hardness and high resistivity. Although relatively high thermal conductivity of bulk BN (1300 Wm⁻¹K⁻¹) [66] has been reported, it is commercially difficult to produce. M.T Alam et al. reported on thermal conductivity of BN thin film to be ≈ 100 Wm⁻¹K⁻¹ in the form of thin film [67].

3.3 Chemical Vapour Deposition (CVD)

Chemical Vapour Deposition Process (CVD) is a deposition process where chemical precursors are transported in the vapour phase to decompose on a heated substrate to form a stable solid product which is usually film [68]. The films that had been coated may be epitaxial, polycrystalline or amorphous depending on the materials and reactor conditions. This method has become the major method of film deposition for the semiconductor industry due to its high throughput, high purity, and low cost of operation [69].

3.3.1 CVD System

In various areas of CVD technology, there is a very large range of reactors and several different precursor delivery systems have been used. This sub-chapter will describe the general overview of CVD system. Irrespective of the variations in CVD processes, all thermal CVD system has the common features [70], such as:

- i) Reactor with reaction zone(s) usually within an enclosed cell, which is heated by a surrounding heating elements, or by external radiofrequency or infrared radiation.
- ii) Gas controller system to control input flow rate of precursor gases or vapours into the reactor.
- iii) Precursor delivery system for various forms of precursors.
- iv) A vacuum pump to evacuate the air and moisture and also for low pressure operation.
- v) An exhaust system which may include an active pump to remove waste by-products efficiently and a waste treatment facility.

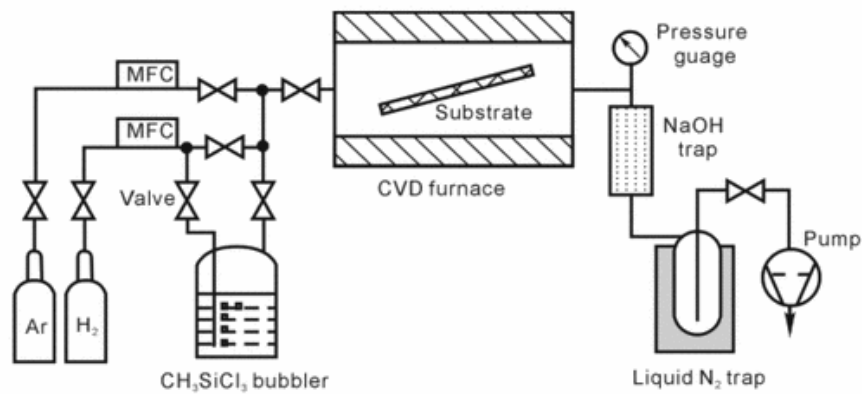


Figure 3.1 Typical set-up of a CVD system [71]

Fig 3.1 shows a typical set-up example of a CVD system. The precursor vapour is delivered by carrier gas into the reactor or furnace. As it passes through the zones with respective temperature, the precursor vapour comes in contact with the substrate and reacts to form a solid film on the surface of the substrate [72].

The reaction kinetics that take place during the CVD process in the reactor are shown graphically in Fig. 3.2. The sequence of events during the reaction is summarized as follows [73]:

- i) Precursor vapours enter into the reactor by mass transport of carrier gas.

- ii) The reactants of the vapours diffuse through the boundary layer to the substrate surface. Intermediates may be formed by homogeneous chemical reactions of precursor during the diffusion.
- iii) Absorption of reactants or intermediates on substrate surface and deposition reaction takes place on surface in solid film growth.
- iv) Desorption of by-products of the reaction from the surface.
- v) Mass transport of by-product in the main flow region away towards the exhaust.

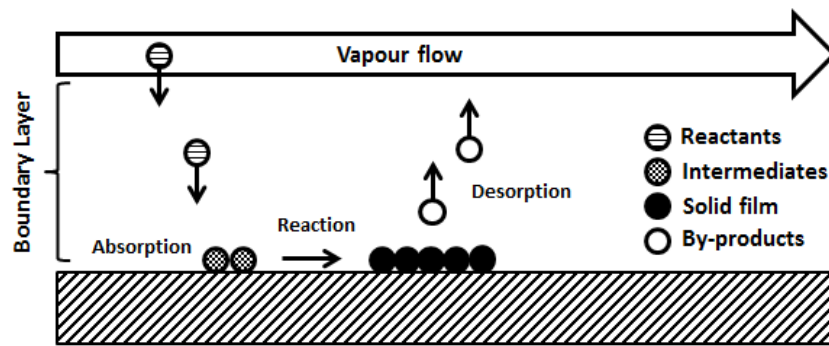


Figure 3.2 CVD reaction kinetics of in reaction zone

3.3.2 Precursor Consideration

In order to obtain the desired material from the deposition process, there are some ideal characteristics or criteria that must be considered, such as:

- i) Low vaporization temperature and sufficient volatility
- ii) High stability at relative low temperatures
- iii) High safety
- iv) Low cost
- v) Chemical purity
- vi) Able to dissolve easily in inert solvents
- vii) Able to react without producing side or parasitic reactions
- viii) Able for being produced in very high degree purity

- ix) Stable under ambient conditions (unaffected by air or moisture), and so forth.

In precursor delivery system, three types of precursors should be considered. The first is the gaseous type, which are source gases in the gaseous state at atmospheric pressure and ambient temperature. It must be diluted with other inert gases to avoid safety problems. It also must be ensured that there is no chemical reaction with equipment to minimize corrosion problem. The second type is liquid precursor, which is usually being heated for vaporization. It involves three methods to deliver the liquid precursors such as direct vaporization, carrier gas sweeping and bubbling. For the solid precursors, it must be heated up to their respective vaporization temperatures in order to activate the reactants [70].

3.3.3 Precursor Bubbling Method

In CVD process, the precursor delivery method is very important as the flow rate limits the growth of thin film. Liquid precursors are normally delivered into reactor through bubbling method with a bubbler. In this method, an inert gas such as hydrogen or nitrogen is bubbled through the liquid precursor with controlled flow rate and the vapour is transported into the deposition chamber. When the vapour passes over a heated substrate, pyrolytic reaction causes chemical decomposition and subsequently produces solid films. This method is generally used because it is an easier and reliable method to obtain a uniform mixture of gases immediately [74]. The flow mechanism of bubbling method is shown in Fig. 3.3.

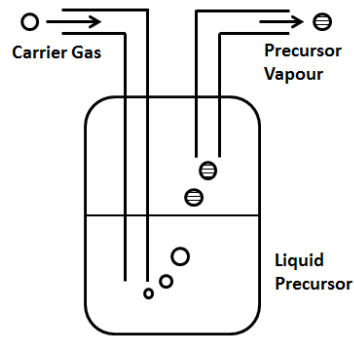


Figure 3.3 The flow mechanism of liquid precursor bubbler

3.4 Principle of 1-D Heat Transfer

The principle of one dimensional (1-D) heat transfer can be explained by heat model as shown in Fig. 3.4.

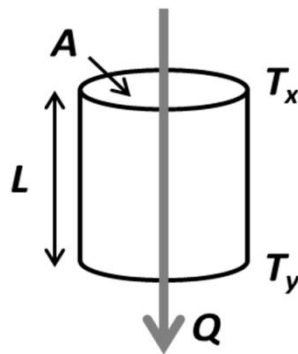


Figure 3.4 One dimension heat transfer across a material

According to Fourier's Law of heat conduction [75-77], the scalar equation is simplified to be:

$$Q = -kA \frac{\delta T}{\partial L} \quad (3.1)$$

Where Q is the heat flow through cross-sectional area (A) of temperature profile (T) with thermal conductivity (k). The minus sign represent the heat flow down in temperature gradient of two boundaries. By integrating Eq. 3.1, the heat flow equation gives:

$$Q = \frac{kA}{L} (T_x - T_y) \quad (3.2)$$

Since the thermal conductance is (kA / L) and Eq. 3.3 shows the relation between thermal resistance and conductance (C), it can be written as Eq. 3.4:

$$Resistance = \frac{1}{C} \quad (3.3)$$

$$Resistance = \frac{L}{kA} = \frac{(T_x - T_y)}{Q} \quad (3.4)$$

At the contacting surface between two materials, the surfaces are only in contact with one another at certain discrete points. The heat transfer across interface is usually compromised by asperities or air gaps and this is compensated by applying TIM between two surfaces to minimize the contact resistance as shown in Fig. 3.5.

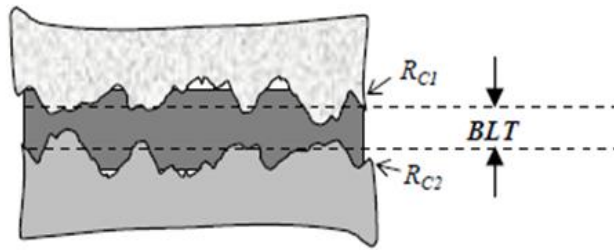


Figure 3.5 TIM applied to fill up the air gaps between two materials [78]

The effective thermal resistance ($R_{effective}$) at the interface can be defined as shown in Eq. 3.5 [78]:

$$R_{effective} = \frac{BLT}{k_{TIM}} + R_{c1} + R_{c2} \quad (3.5)$$

Where BLT is the bond line thickness of TIM, k_{TIM} is the thermal conductivity of TIM, R_{c1} and R_{c2} are contact resistances of TIM at two bounding surface. Eq. 3.5 shows that BLT directly determines the $R_{effective}$ of the interface, therefore considering the thickness of thin film is essential in thermal management.

3.5 Thermal and Optical Relation in Thermal Measurements

The device junction temperature (T_j) of LEDs can be determined by:

$$T_j = T_{j0} + \Delta T_j \quad (3.6)$$

Where T_{j0} is the initial LED junction temperature and ΔT_j is the change in junction temperature due to heat dissipation of LED chip. The relationship between ΔT_j and power dissipation is usually linear depends on some specific conditions, and it may vary considerably at the extremes of LED operation. Thus, the environmental conditions have to be considered to assure the significance of test results.

Thermal resistance (R_{th}) of a device is defined as the capability of the device to transfer heat from initial point to final point. According to JEDEC standard 51-1 [79], R_{th} is defined as in Eq. 3.7.

$$R_{thJX} = \frac{T_j - T_x}{P_H} \quad (3.7)$$

Where R_{thJX} is the thermal resistance from device junction to the specific environment, T_j is the device junction temperature under steady state condition, T_x is the reference temperature for a specific environment or condition and P_H is the power dissipated in the device. The heat dissipation efficiency of LEDs is measured in term of R_{th} and it serves to the determination of T_j that arises in the LEDs under various operating conditions.

In the optical performance of LEDs, the light output of LEDs strongly depends on the operating conditions. As an LED is forward biased, the input electrical power (P_I) is converted into output optical power (P_{opt}) and power of heat dissipation (P_H) [80]. The relation is shown in terms of:

$$P_I = P_{opt} + P_H \quad (3.8)$$

At higher supplied electrical power or current, more light is generated by LEDs. It was reported that optical efficiency achieved can up to 30% of the supplied electrical power [81]. However, when the forward current increases, the temperature gradient is also increases and eventually causes a drop in the light output. The dependence of R_{th} with P_H is redefined as in Eq. 3.9 [82]:

$$R_{th} = \frac{T_j - T_x}{P_I - P_{opt}} \quad (3.9)$$

The real R_{th} values yield by considering the P_{opt} in the calculations according to Eq. 3.9. The lower the R_{th} value, the better is the thermal performance and the device can be protected from overheating.